Romanian Reports in Physics **XX**, XYZ (2017)

EFFECTS OF ELECTRIC, MAGNETIC AND INTENSE LASER FIELDS ON THE ELECTROMAGNETICALLY INDUCED TRANSPARENCY IN A SEMI-PARABOLIC QUANTUM WELL

D. BEJAN[1], C. TRUȘCĂ[2]

[1]*Faculty of Physics, University of Bucharest, Bucharest, Romania,E-mail: doinitabejan@yahoo.com;*
[2]*Physics Department, "Politehnica" University of Bucharest, Romania*

Abstract. The effects of the electric, magnetic, non-resonant intense laser and control laser fields on the electronic and optical properties -absorption coefficient and refraction index- of a $GaAs/Al_{0.3}Ga_{0.7}As$ semi-parabolic quantum well related to the occurrence of the electromagnetically induced transparency phenomenon are investigated. It is found that the electromagnetically induced transparency occurs in the system in all cases but it is advantaged by a proper choice of the external fields. The increase of the non-resonant laser intensity strongly enlarges the transparency window width. Furthermore, the transparency window for absorption of the probe laser is blue-shifted by the augment of the electric or magnetic field strength.

Key words: semiconductor, semi-parabolic quantum well, non-resonant intense laser, static electric field, magnetic field, electromagnetically induced transparency.

1. INTRODUCTION

The electromagnetically induced transparency (EIT) is a special phenomenon in which light is controlled with light. In EIT, the absorption is reduced for a probe laser in the presence of a strong control (pump) laser in a three level system via the destructive interference in absorption of the dressed states that are produced as a coherent superposition of the bare initial states. In the region of reduced absorption is induced a large variation of the linear dispersion that determines the slowing down of the group velocity of light [1]. The study of slow light process is of great interest, having wide applications in creating of optical buffers [2], quantum information processing [3], optical switches [4,5] and low-light level optical devices [6]. EIT has been observed in neutral strontium [7], lead vapors [8], ultra-cold sodium vapors [9], rare-earth-ion doped crystals [10], semiconductor quantum wells [11-15] and quantum dots [16].

Quantum wells (QWs) and quantum dots are excellent candidates for investigation of EIT. The quantum confinement of the carriers in these structures leads to the discretization of the energy levels, providing a discrete three-level system for EIT occurrence [17-24].

In the present work we investigate the electromagnetically induced transparency in a $GaAs/Al_{0.3}Ga_{0.7}As$ semi-parabolic quantum well subjected to external electric, magnetic and non-resonant intense laser fields. To the best of our knowledge, this system has not been studied theoretically before in view of EIT occurrence even its nonlinear optical properties were largely studied (see for example [25] and references therein).

The outline of the paper is as follows. In Section 2 we describe the theoretical framework. The numerical results are presented and discussed in Section 3. A brief summary is given in Section 4.

2. THEORY

2.1 SEMI-PARABOLIC QW UNDER ELECTRIC, MAGNETIC AND NON-RESONANT INTENSE LASER FIELDS

We consider a GaAs semi-parabolic QW grown along the z-direction, embedded between $Al_{0.3}Ga_{0.7}As$ barriers of height V_0 (in the regions $z \le 0$ and $z \ge L$). The heterostructure is submitted to the joint action of electric and/or magnetic fields and an intense laser radiation. According to the effective mass theory, in the absence of the laser field, the Hamiltonian for the confined electron in the structure can be written as:

$$H = \frac{1}{2m^*}\left(\vec{p} + e\vec{A}\right)^2 + V(z) + eFz \,. \tag{1}$$

The first term of the Hamiltonian is the kinetic energy of the electron under the influence of the magnetic field $\vec{B}$, m^* is the electron effective mass, e is the elementary charge, $\vec{p}$ is the electron momentum operator, $\vec{A}$ is the vector potential of the magnetic field and F is the amplitude of the electric field oriented along the growth direction. $V(z)$ is the semi-parabolic potential:

$$V(z) = \begin{cases} V_0 & z \le 0 \cup z \ge L \\ V_0 z^2 / L^2 & 0 < z < L \end{cases}. \tag{2}$$

Taking the magnetic field parallel with the *x* direction, $\vec{B} = B\hat{x}$ and using the non-symmetric gauge $\vec{A} = -Bz\hat{y}$, the Hamiltonian in the *z* direction reduces to:

$$H = -\frac{\hbar^2}{2m^*}\frac{\partial^2}{\partial z^2} + V(z) + \frac{e^2B^2z^2}{2m^*} + eFz. \tag{3}$$

In order to consider the effects of a non-resonant laser field (NLF, a laser of energy close to GaAs band gap), represented by a monochromatic plane wave which is linearly polarized along *z*-axis, we use the Floquet method. In the high-frequency limit [26-28] the electron "sees" a laser-dressed confinement potential,

$$\tilde{V}_{eff}(z,\alpha_0) = \frac{\omega_L}{2\pi}\int_0^{2\pi/\omega_L} V_{eff}(z+\alpha(t))\,dt \tag{4}$$

where

$$V_{eff}(z) = V(z) + \frac{e^2B^2z^2}{2m^*}. \tag{5}$$

$\alpha(t) = \alpha_0 \sin(\omega_L t)$ describes the motion of the electron in the laser field and $\alpha_0 = \frac{eA_{0L}}{m^*\omega_L}$ is the laser-dressing parameter [26]. Here ω_L and A_{0L} are the angular frequency and the vector potential amplitude of NLF.

The dressed potential has the analytical expression [29]:

$$\tilde{V}_{eff}(z,\alpha_0) = \begin{cases} V_0 + \frac{e^2B^2}{2m^*}\left(z^2 + \alpha_0^2/2\right) & z \le -\alpha_0 \cup z \ge L + \alpha_0 \\ \left(\frac{V_0}{L^2} + \frac{e^2B^2}{2m^*}\right)\left(z^2 + \alpha_0^2/2\right) + \frac{V_0}{\pi}\arccos\left(\frac{z}{\alpha_0}\right)\left(1 - \left(z^2 + \alpha_0^2/2\right)/L^2\right) + \frac{3V_0 z}{2\pi L^2}\sqrt{\alpha_0^2 - z^2} & -\alpha_0 < z \le \alpha_0 \\ \left(\frac{V_0}{L^2} + \frac{e^2B^2}{2m^*}\right)\left(z^2 + \alpha_0^2/2\right) & \alpha_0 < z \le L - \alpha_0 \\ \left(\frac{V_0}{L^2} + \frac{e^2B^2}{2m^*}\right)\left(z^2 + \alpha_0^2/2\right) + \frac{V_0}{\pi}\arccos\left(\frac{L-z}{\alpha_0}\right)\left(1 - \left(z^2 + \alpha_0^2/2\right)/L^2\right) & \\ \quad - \frac{V_0}{\pi L^2}\left(\frac{L+3z}{2}\right)\sqrt{\alpha_0^2 - (L-z)^2} & L - \alpha_0 < z < L + \alpha_0 \end{cases}$$

The electronic states of the well may be obtained by numerically solving a 1D Schrödinger equation for the dressed Hamiltonian:

$$H_d = -\frac{\hbar^2}{2m^*}\frac{\partial^2}{\partial z^2} + \tilde{V}_{eff}(z,\alpha_0) + eFz. \quad (6)$$

2.2 EIT IN A THREE-LEVEL SYSTEM

With the calculated wave-functions ψ_i we can now compute the transition moments $\mu_{ij} = \langle \psi_i | z | \psi_j \rangle$. As we will prove in the following, the transition $1 \to 3$ has a very low transition moment, whereas the excited state $|2\rangle \equiv \psi_2$ has a nonzero electric dipole coupling to both $|1\rangle \equiv \psi_1$ and $|3\rangle \equiv \psi_3$ states. These characteristics define a three-level system in a ladder-type Ξ-configuration.

In order to obtain the electromagnetically induced transparency, a pair of near-resonant laser fields with *z*-polarization is coupled to the system. For the Ξ-configuration, the probe laser of frequency ω_p and amplitude $\vec{E}_p$ drives the $1 \to 2$ transition. The $3 \to 2$ transition, having the resonant frequency $\omega_{32} = (E_3 - E_2)/\hbar$, is driven by the control laser having the frequency ω_c and the amplitude $\vec{E}_c$. The probe and control lasers are detuned from the resonance frequencies by $\Delta_p = \omega_{21} - \omega_p = (E_2 - E_1)/\hbar - \omega_p$ and $\Delta_c = \omega_{32} - \omega_c$, respectively.

The interaction Hamiltonian is:

$$H_{\text{int}}(t) = -e\vec{\mu} \cdot \vec{E} \quad (7)$$

with $\vec{\mu}$ the electric dipole moment operator and $\vec{E}$ the electric field amplitude of the applied laser pulses:

$$\vec{E}(\vec{r},t) = \frac{\vec{E}_p}{2}\left[\exp(i\omega_p t) + \exp(-i\omega_p t)\right] + \frac{\vec{E}_c}{2}\left[\exp(i\omega_c t) + \exp(-i\omega_c t)\right] \quad (8)$$

In the rotating-wave approximation [30], we can represent the Hamiltonian of the three-level Ξ-system interacting with the applied laser pulses as:

$$H = -\hbar\begin{bmatrix} 0 & \Omega_p & 0 \\ \Omega_p & -\Delta_p & \Omega_c \\ 0 & \Omega_c & -(\Delta_p + \Delta_c) \end{bmatrix}. \quad (9)$$

where Ω_p and Ω_c are half of the Rabi frequencies [30] and are defined as:

$$\Omega_p = \frac{\Omega_p^R}{2} = \frac{e\mu_{12}E_p}{2\hbar},\ \Omega_c = \frac{\Omega_c^R}{2} = \frac{e\mu_{23}E_c}{2\hbar}\ . \tag{10}$$

Here μ_{21} and μ_{23} are the dipole moment matrix elements associated with the transition driven by the probe laser and the control laser, respectively.

The susceptibility of the three-level system induced by the probe and control lasers is [20,24]:

$$\chi = \frac{Ne^2\mu_{12}^2}{\varepsilon_0\hbar}\frac{-\delta + i\gamma_{31}}{\Omega_c^2 + (\gamma_{21} + i\Delta_p)(\gamma_{31} + i\delta)}, \tag{11}$$

where N is the density of the 3-level system , $\delta = \Delta_p + \Delta_c$ and γ_{ij} are the decay rate between the states i and j composed from the radiative decay rate due to the spontaneous emission and the dephasing rate [1].

The above complex susceptibility gives rise to a complex refraction index [24] with real and imaginary parts that read as:

$$n_T = \sqrt{\frac{n_r^2 + \mathrm{Re}(\chi) + \sqrt{(n_r^2 + \mathrm{Re}(\chi))^2 + \mathrm{Im}(\chi)^2}}{2}}, \qquad \kappa = \frac{\mathrm{Im}(\chi)}{2n_T} \tag{12}$$

where n_r is the static refractive index of the material. The absorption coefficient is related to the imaginary part of the susceptibility [30]:

$$\alpha(\omega) = \frac{2\omega\kappa}{c} = \frac{\omega\,\mathrm{Im}(\chi)}{cn_T} = \frac{\omega Ne^2\mu_{12}^2}{\varepsilon_0\hbar cn_T}\frac{\gamma_{21}(\gamma_{31}^2 + \delta^2) + \gamma_{31}\Omega_c^2}{(\Omega_c^2 + \gamma_{21}\gamma_{31} - \Delta_p\delta)^2 + (\Delta_p\gamma_{31} + \delta\gamma_{21})^2}. \tag{13}$$

3. RESULTS AND DISCUSSION

The present paper investigates the realization of the electromagnetically induced transparency in GaAs/$Al_{0.3}Ga_{0.7}As$ quantum well under external fields through the related optical properties: absorption coefficient and refraction index. The parameters used in our calculations are: $V_0 = 228$ meV, L=25 nm [29], $m^* = 0.067m_0$ (where m_0 is the mass of a free electron), $N = 3x10^{22}$ m^{-3}, $n_r = 3.55$ [29], $\gamma_{31} = \gamma_{21} = 5x10^{11}$ Hz [24]. We use a discrete variable

representation technique [31-33] to solve the Schrödinger equation for Hamiltonian (6).

3.1 ELECTRONIC PROPERTIES

In Fig. 1a we represent the dressed potential of the semi-parabolic quantum well in the presence of the electric, magnetic and intense laser fields. We observe that, for a positive oriented electric field, the effective width of the QW is decreased and the right and left barriers are increased/decreased. The applied magnetic field determines a stronger decrement of the well width than the electric field and an increment of the left and right barriers that take now a parabolic form. The effect of the non-resonant laser is to increase the width of the upper part of the dressed potential and the minimum value of the potential, while the width of the bottom part decreases.

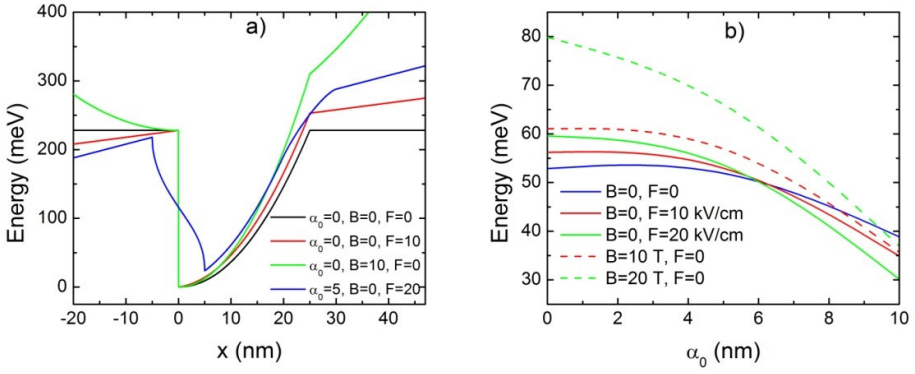

Fig. 1 a) The dressed potential of the semi-parabolic QW and b) the transition energy E_{21} as function of the laser parameter α_0 for different values of the external fields.

The displacement of the potential well toward higher values induced by the NLF leads to the increment of all levels of energy but also the levels get closer. Therefore the transitions energies are reduced with NLF strengthening. The increase of the potential confinement induced by the electric and magnetic fields determines an augment of the energy levels and a better separation between them. Thus the effect of the electric and magnetic fields is to increase the transition energies for low values of the NLF parameter. At larger values of this parameter the enlargement of the well induced by the NLF compensates the narrowing produced by the electric or magnetic fields and the energy is decreased. These characteristics are obvious in Fig. 1b where the transition energy $E_{21}=E_2-E_1$ is showed.

The transition moments are represented in Fig. 2 function of the laser parameter for different values of the electric and magnetic fields. In Fig. 2a we

observe that the moments for $1 \to 2$ and $2 \to 3$ transitions increase with the NLF strengthening. The electric and magnetic fields clearly influence their values, the magnetic field having a stronger influence. The moments for the $1 \to 3$ transition are very low in comparison with μ_{12}, μ_{23} and can be made practically zero with the proper choice of the external fields as can be seen in Fig. 2b. As demonstrated in [7], the condition of reduced absorption in the $1 \to 2$ transition is that, at the application of the probe and control lasers, the ground state $|1\rangle$ evolves into a steady state where a fraction of the population is in state $|3\rangle$. If $|3\rangle$ is a metastable state, the absorption is reduced by the destructive interference of the dressed states (created by the control laser). To this end μ_{13} must be close to zero. If the semi-parabolic well were infinite then $1 \to 3$ transition would be strictly forbidden. But as the barrier height for GaAs/$Al_{0.3}Ga_{0.7}$As system is finite ($V_0 = 228$ meV [29]) one have to find a way of lowering μ_{13} using the external fields. This situation is produced at α_0=5 nm, B=10 T, F=20 kV/cm and at α_0=10 nm, B=20 T, F=20 kV/cm.

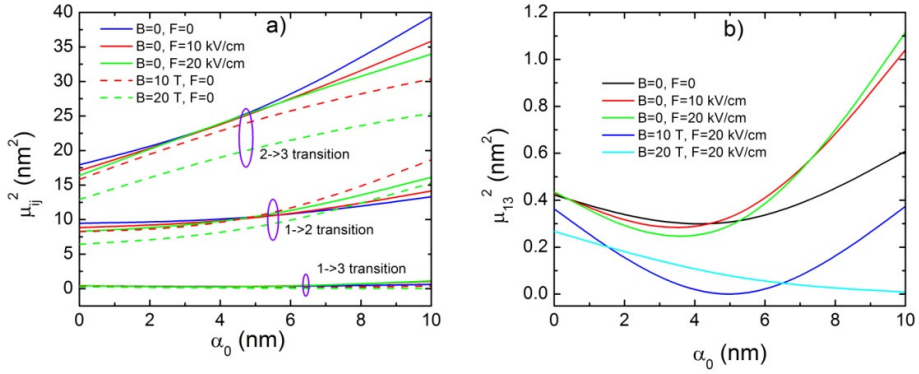

Fig. 2 a) The transition moments and b) μ_{13}^2 as function of the laser parameter α_0 for different values of the external fields.

3.2 OPTICAL PROPERTIES

In this section we present the effects of the electric, magnetic, non-resonant intense laser fields and control laser on the optical properties of the GaAs/$Al_{0.3}Ga_{0.7}$As quantum well related to the occurrence of the electromagnetically induced transparency phenomenon. To this end, we illustrate

in Figs. 3-6 the absorption coefficient (AC) and the refraction index (RI) as a function of the probe laser frequency ω_p for different values of the external fields.

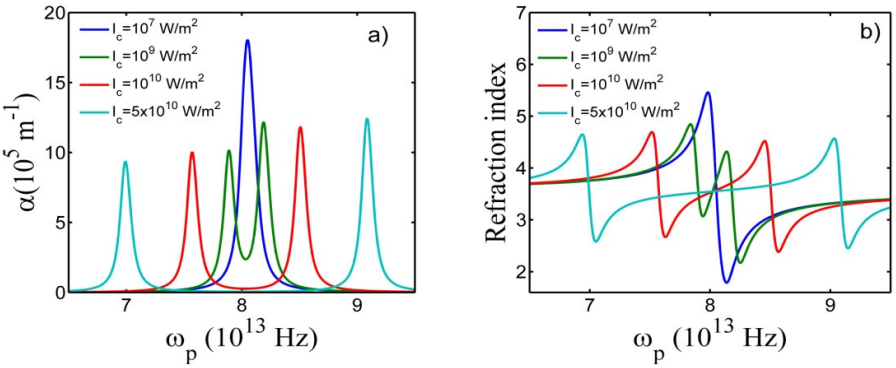

Fig. 3 a) The absorption and b) the refraction index as function of the probe frequency at four values of the control laser intensity.

We begin our analysis with a discussion on the effect of the intensity of the control laser that is applied on the QW in the absence of electric, magnetic and NLF fields. In this case, μ_{12}=3.075 nm, μ_{13}=0.649 nm and μ_{23}=4.233 nm, so $\mu_{13} << \mu_{12}, \mu_{23}$ and EIT can occur. As can be seen in Fig. 3a, at low intensity of the control laser (I_c=10^7 W/m^2 or lower) the absorption has a Lorentzian profile with maximum at $\omega_p = \omega_{21}$ if $\Delta_c = 0, \delta = \Delta_p$ so the transparency cannot be induced. The refraction index has a negative slope (anomalous dispersion) in the narrow region centered on $\omega_p = \omega_{21}$ (see Fig. 3b). At larger intensities, the absorption presents two unequal maxima and a minimum at $\omega_p = \omega_{21}$ if the following condition is fulfilled [20,24]:

$$\Omega_c > \frac{\gamma_{31}\sqrt{\gamma_{31}}}{\sqrt{\gamma_{21}+2\gamma_{31}}} . \qquad (14)$$

The control laser intensity is related to Ω_c by $I_c = \frac{\varepsilon_0 c n_r E_c^2}{2} = \frac{2\hbar^2 \varepsilon_0 c n_r \Omega_c^2}{e^2 \mu_{23}^2}$. However, we observe that even at I_c=10^9 W/m^2 the transparency is still not perfect, the absorption having a residual value. At I_c=5x10^{10} W/m^2 we can say that the transparency is quite good, because in this case, the condition of EIT occurrence $\alpha_{\min} \le 10^{-3}\alpha_{Max}$ is respected [18]. Here

α_{Max}, $\alpha_{\min}$ are the values of the absorption maximum in the absence of the control laser $\alpha_{Max} = \frac{\omega_{21} N e^2 \mu_{12}^2}{\varepsilon_0 \hbar c n_T} \frac{1}{\gamma_{21}}$ and absorption minimum at the present control laser intensity $\alpha_{\min} = \frac{\omega_{21} N e^2 \mu_{12}^2}{\varepsilon_0 \hbar c n_T} \frac{\gamma_{31}}{\Omega_c^2 + \gamma_{21}\gamma_{31}}$ [24]. For $\Delta_p = 0$ (zero detuning of the probe field) and $\Omega_c >> \gamma_{21}, \gamma_{31}$ the magnitudes of the two peaks are [24]:

$$\alpha_{\max}^{\pm} = \frac{N e^2 \mu_{12}^2}{\varepsilon_0 \hbar c n_T} \frac{\omega_{21} \pm \Omega_c}{\gamma_{21} + \gamma_{31}}. \qquad (15)$$

The two peaks are unequal due to the different signs of Ω_c in the numerator of Eq. (15) and are separated by a transparency windows (*TW*) centered on $\omega_p = \omega_{21}$, having the value $TW \approx 2\Omega_c$. At I_c=5x10^{10} W/m^2, the amplitude of the control laser is rather low, E_c = 3.26x10^6 V/m, and Ω_c =1.047x10^{13} Hz, ensuring a rather large TW. The transparency window corresponds to a positive slope in RI (normal dispersion) that decreases at the augment of Ω_c.

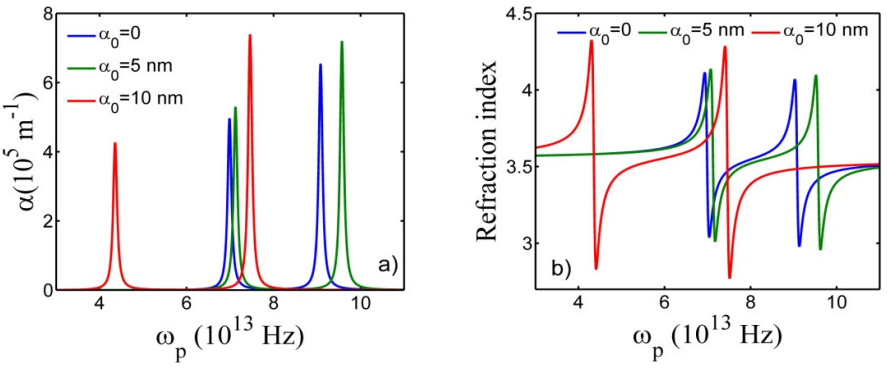

Fig. 4 a) The absorption and b) the refraction index as function of the probe frequency for three values of the NLF parameter, at B=0 and F=0.

In order to see the effect of the external fields on the semi-parabolic well we represent in Figs. 4-6 the AC and RI at the same value of the control laser intensity I_c=5x10^{10} W/m^2.

In Fig. 4 we depict the AC and RI for three values of the NLF parameter α_0 in the absence of the electric and magnetic fields. Some effects are noticeable

in Fig. 4 at the augment of α_0: i) the AC and RI peaks increase due to the μ_{12} increment (see Fig. 2a); ii) the TW value increases according to the μ_{23} raise that induces the augment of Ω_c; iii) the TW goes first to higher probe frequencies at α_0<5 nm and then toward lower probe frequency in agreement to the behavior of the transition energy E_{21} observed in Fig. 1b. Note that $\alpha_{\min}$ decreases at the increment of Ω_c, thus the condition $\alpha_{\min} \le 10^{-3}\alpha_{Max}$ is always respected.

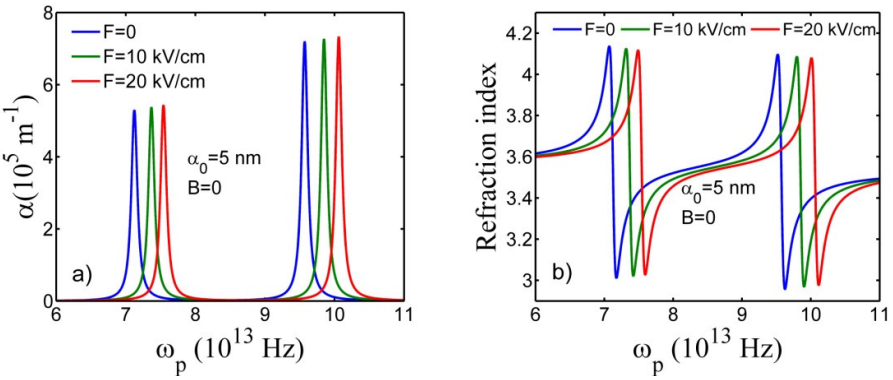

Fig. 5 a) The absorption and b) the refraction index as function of the probe frequency for three values of the electric field for α_0=5 nm and B=0.

In fig. 5 we illustrate the AC and RI at different values of the electric field, in the presence of NLF but in the absence of the magnetic field. We choose the NLF parameter to be α_0=5 nm because in this case the transition moment μ_{13} has a minimum and the EIT occurrence is favored. We observe that the width of the transparency windows is almost constant because μ_{23} remains quasi-constant for this particular choice of external fields, but is blue-shifted at the electric field strengthening due to the raise of the transitions energy E_{21} seen in Fig. 1b. The E_{21} raise also determines the slight increment of the AC peaks due to ω_{21} appearance in the numerator of Eq. (15).

In order to see the influence of the magnetic field on the EIT characteristics we represent in Fig. 6 the AC and RI at different values of the magnetic field for the NLF parameter α_0=5 nm. The electric field is absent for the blue and green curves but is set to F=20 kV/cm for the red curve because for this choice of parameters $\mu_{13} = 0.015$ nm favoring the EIT occurrence in the semi-parabolic well. As in Fig. 5, the most interesting effect is the blue-shift of the transparency windows caused by E_{21} increment with B (and with F at the same B)

seen in Fig. 1b. The peaks magnitude and *TW* width are almost constant for F or B variation at α_0=5 nm. The transparency window width will be strongly increased (decreased) by the augment (diminution) of the NLF intensity.

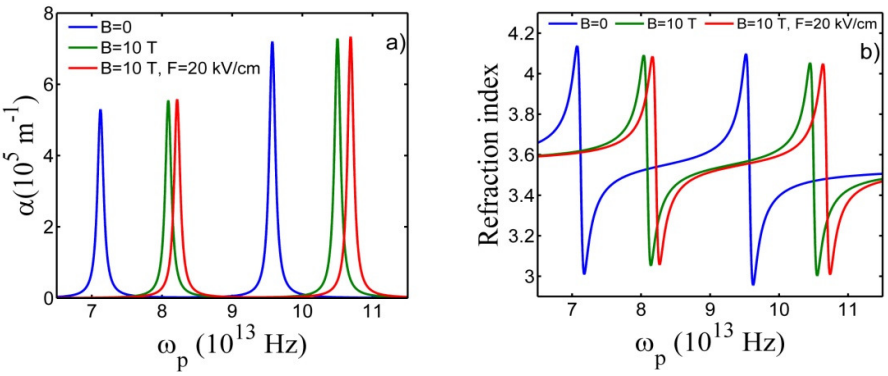

Fig. 6 a) The absorption and b) the refraction index as function of the probe frequency for two values of the magnetic field and α_0=5 nm.

4. CONCLUSIONS

In this work we investigate the electromagnetically induced transparency in a GaAs/$Al_{0.3}Ga_{0.7}As$ semi-parabolic quantum well subjected to external electric, magnetic and non-resonant intense laser fields. Our main findings are: i) the EIT occurs in the system in all cases but it is advantaged by a proper choice of the external fields; ii) the increase of the non-resonant laser intensity strongly enlarges the transparency window width; iii) the transparency window for absorption of the probe laser is blue-shifted by the augment of the electric or magnetic field strength. The system allows a rather large transparency window at rather low amplitude of the control laser. The results obtained in our study can be used to design new optical devices based on the EIT phenomenon.

REFERENCES

1. M. Fleischhauer, A. Imamoğlu, J. P. Marangos, Rev. Mod. Phys. **77**, 633-673 (2005).
2. P. C. Ku, S. Forrest, C. J. Chang-Hasnain, P. Phedon, Li Tao,W. Hailin,C. Shu-Wei,C. Shun-Lien, Opt. Lett. **29**, 2291–2293 (2004).
3. R. G. Beausoleil, W. J. Munro, D. A. Rodrigues, T. P. Spiller, J. Mod. Opt. **51**, 2441-2448 (2004).
4. S. Zhang, S. Zhou, M.M.T. Loy, G.K.L. Wong, S. Du, Opt. Lett. **36**, 4530–4532 (2011).
5. S.E. Harris, Y. Yamamoto, Phys. Rev. Lett. **81**, 3611-3614 (1998).

6. S.E. Harris, L. V. Hau, Phys. Rev. Lett. **82**, 4611-4614 (1999).
7. K.J. Boller, A. Imamoglu, S. Harris, Phys. Rev. Lett. **66**, 2593–2596 (1991).
8. J. E. Field, K. H. Hahn, and S. E. Harris, Phys.Rev. Lett. **67**, 3062-3065 (1991).
9. L.V. Hau, S.E. Harris, Z. Dutton, C.H. Behroozi, Nature **397**, 594–598 (1999).
10. B.S. Ham, P.R. Hemmer, M.S. Shahriar, Opt. Commun. **144**, 317-130 (1997).
11. G.B. Serapiglia, E. Paspalakis, C. Sirtori, K.L. Vodopyanov, C.C. Phillips, Phys. Rev. Lett. **84**, 1019–1022 (2000).
12. S.-M. Ma, H. Xu, B. S. Ham, Opt. Express **17**, 14902-14908 (2009).
13. S. Hanna, B. Eichenberg, D. A. Firsov, L. E. Vorobjev, V. M. Ustinov, Phys. E **75**, 93-96 (2016).
14. M. C. Phillips,H.Wang, Phys. Rev. B **69**, 115337 (2004).
15. H. Kang, J. S. Kim, S.I. Hwang,Y. H. Park, D. Ko, J. Lee, Opt. Express **16**, 15728– 15732 (2008).
16. S. Marcinkevičius, A. Gushterov, J. P. Reithmaier, Appl. Phys. Lett. **92**, 041113 (2008).
17. Z. Raki, H. R. Askari, Superlatt. Microstruct. **65**, 161-176 (2014).
18. H. R. Askari, Z. Raki, Superlatt. Microstruct. **71**, 82-92 (2014).
19. B. Vaseghi, N. Mohebi, J. Lumin. **134**, 352-357 (2013).
20. V. Pavlović, L. Stevanović, Superlatt. Microstruct. **92**, 10-23 (2016).
21. G. Rezaei, S. Shojaeian Kish, B. Vaseghi, S. F. Taghizadeh, Phys. E **62**, 104-110 (2014).
22. E. C. Niculescu, Opt. Mat. **64**, 540-647 (2017).
23. D. Bejan, Opt. Mat. **67**, 145-154 (2017).
24. D. Bejan, Eur. Phys. J. B **90**, 54 (2017).
25. D. Bejan, Eur. Phys. J. Plus **132**, 102 (2017).
26. M. Gavrila, J.Z. Kaminski, Phys. Rev. Lett. **52,** 613-616 (1984).
27. M. Gavrila, *Lecture Notes in Physics, Fundamentals of laser interactions*, Vol. 229, Springer, Berlin, 1985.
28. M. Pont, N.R. Walet, M. Gavrila, C.W. McCurdy, Phys. Rev. Lett. **61,** 939-942 (1988).
29. F. Ungan, J.C. Martínez-Orozco, R.L. Restrepo, M.E. Mora-Ramos, E. Kasapoglu, C.A. Duque, Superlatt. Microstruct. **81,** 26-33 (2015).
30. R. Loudon, The quantum theory of light, 2end ed., Clarendon Press, Oxford, 1988.
31. J. V. Lill, G. A. Parker, J. C. Light, Chem. Phys. Lett. **89**, 483-489 (1982).
32. J.C. Light, I. P. Hamilton, J. V. Lill, J. Chem. Phys. **82**, 1400-1409 (1985).
33. D. T. Colbert, W. H. Miller, J. Chem. Phys. **96**, 1982-1991 (1992).